Phase Transitions of Phospholipid Monolayers Penetrated by Apolipoproteins

J. Xicohtencatl-Cortes,† Jaime Mas-Oliva,† and Rolando Castillo*,‡

Instituto de Fisiología Celular, UNAM, Apdo. Postal 70-243, México D. F. 04510, and Instituto de Física, UNAM, Apdo. Postal 20-364, México D. F. 01000

Received: October 1, 2003; In Final Form: February 20, 2004

Experiments for adsorbing apolipoproteins (CI and AII) on a phospholipid (DPPC, *rac*-1,2-dipalmitoyl-*sn*-glycero-3-phosphocholine) monolayer were made. Our results indicate that lipoproteins in fact did not adsorb underneath the DPPC monolayer; instead lipoproteins actually penetrate the DPPC monolayer to form part of the monolayer at the air/water interface. The binary monolayers were isothermically compressed and their textures observed with Brewster angle microscopy. These monolayers that are rich in DPPC present two clear first-order phase transitions between condensed phases, as well as one between a condensed phase and a gas phase. At very high lateral pressures, condensed domains rich in protein present a high reflectivity. These domains melt away as pressure increases, leaving them indistinguishable from the rest of the low-reflectivity optically isotropic monolayer. Apparently, they lose density or thickness as if proteins were expelled from the air/water interface. A model for understanding the phase transitions in these binary systems is presented, which could have important implications in the understanding of lipoprotein physiology.

Introduction

Important molecules such as cholesterol, triglycerides, and phospholipids that are mostly water insoluble are transported in plasma and mobilized to and from cells throughout lipoprotein particles. Some proteins associated with these particles are known as apolipoproteins (APOs). They apparently give lipoproteins directionality and the ability to interact with receptors at the surface of cells.[1] Several of these APOs can exchange among the different classes of lipoproteins particles, while others form part of the particles as fixed proteins.[2,3] Exchangeable APOs are protein constituents of high-density lipoproteins (HDL).[1] HDL are the mediators for the reverse cholesterol transport, a process that removes excess cholesterol from cell membranes of peripheral tissues resulting in protection against arteriosclerosis.[1,4−7] Exchangeable APOs, which are membrane active proteins, are generally built of hydrophilic and hydrophobic peptides, which form sequences with highly amphiphilic secondary structural motives. When such proteins are in contact with a biphasic media (polar/nonpolar), their tendency is to anchor their hydrophilic and hydrophobic regions in the polar and the nonpolar media, respectively. Hence, a hydrophobic/hydrophilic interface tends to induce a specific orientation on the adsorbed molecules. Models of lipoprotein particles[8] are basically spheres made of a phospholipid monolayer filled with triglycerides and cholesterol esters, where the phospholipids heads are in contact with the plasma. In these models, APOs are usually placed lying down on the lipoprotein particles.[8,9]

Understanding how the APOs perform their biological function at the surface of the lipoprotein particles has been a lengthy pursued aim, still waiting for answers. Our group has studied the physicochemical behavior of APOs at the air/water interface, as a model for hydrophobic/hydrophilic interfaces, employing monolayers. Exchangeable APOs present no similarities in their primary structure.[10] However, at a secondary structure level, important similarities appear, mainly due to the presence of amphipathic α-helices as their main structural motive.[10−12] The amphiphilic character of apolipoproteins is based on the fact that a polar protein face is formed due to the clustering of charged amino acid residues on one side, whereas a hydrophobic surface composed of nonpolar residues is formed at the opposite face of the α-helix.[10−12] Hydrophobic moment calculations have confirmed the amphiphilic character of APO α-helices.[10−12] APO CI is composed of 57 amino acid residues in length, with a molecular mass of 6.63 kDa. Two crystalline forms of APO CI have been reported as suitable for high-resolution X-ray diffraction analysis.[13] However, its three-dimensional structure still remains unsolved. Secondary structure predictions, nuclear magnetic resonance, and circular dichroism studies made on APO CI have revealed a high α-helix content, distributed in two α-helices.[14−16] The first α-helix (residues 4−30) presents approximately 7.5 periods (a period = 3.6 amino acids of 5.4 Å pitch), while the second one (residues 35−53) consists of 5.2 periods. APO AII is a protein formed by two identical polypeptide chains bonded by a disulfide bridge at position 6, where each chain corresponds to 77 amino acid residues in length, and a molecular mass of 8.708 kDa.[17] Its three-dimensional structure also remains unsolved. Predictive studies have shown that each chain of the APO AII also presents two α-helix motifs (peptides encompassing 7−27 and 32−67) as its main secondary structure.[11] When APO CI and APO AII are deposited onto a highly ionic water subphase to form a monolayer, two first-order phase transitions are found on compression.[11,12] The first one involves a condensed fluid phase, which has been denoted as L, coexisting with a low-density gaseous phase (G), where proteins are weakly interacting. The second phase transition involves two condensed phases, the L phase and the LC phase.[11,12] This transition occurs for APO CI at $\Pi \sim 33$ mN m^{-1} and $A \sim 350-600$ Å^2 molecule^{-1}, and for APO AII at 30−35 mN m^{-1} and $A = 1000-2500$ Å^2

* To whom correspondence should be addressed. E-mail: rolandoc@fisica.unam.mx.
† Instituto de Fisiología Celular.
‡ Instituto de Física.

10.1021/jp0369443 CCC: $27.50
Published on Web 04/29/2004

molecule^{-1}. A model for both proteins at the air−water interface has been suggested, where APO CI is modeled as two-amphiphilic α-helices bonded by a loose hinge[12] and APO AII as two-amphiphilic chains bonded at position 6. Here, each chain has two α-helices, also bonded by a loose hinge.[11] The second phase transition in both proteins is due to a conformational change, where one α-helix segment in the case of APO CI[12] or two α-helix segments in the case of APO AII[11] desorb from the subphase. Direct evidence of these conformational changes have been shown using grazing incidence X-ray diffraction and scanning Langmuir−Blodgett of transferred monolayers with atomic force microscopy (AFM).[18]

Isothermal compression of phospholipid monolayers typically produces a sequence of two-dimensional (2D) phases as density increases, starting with a gas (G) phase, a liquid expanded (LE) phase, a tilted condensed (TC) orientationally ordered phase, and an untitled condensed (UC) positionally ordered phase.[19] The TC and UC phases were formerly labeled as liquid condensed and solid, although this last phase is not shown in the particular case of DPPC (*rac*-1,2-dipalmitoyl-*sn*-glycero-3-phosphocholine). Here, the tilting of the alkyl chains is 37°−29° in the TC phase,[20] and the three methyl groups in its big head (∼45 Å^2) prevents a vertical tail arrangement. In phospholipids, phases with free chain rotation along the molecular axes should not exist, since the coupling of two chains prevents rotation. Lateral motion of a molecule requires the movement of two chains, which is hindered, thus reducing the role of translational freedom compared to the internal degrees of freedom of a molecule. Position and orientation of the headgroups can also be involved in ordering, and the interactions between the headgroups can be laterally anisotropic. Until now, X-ray experiments have revealed the order of the aliphatic tails, but not that of the headgroups.[19] In the literature, many studies have been made using DPPC monolayers, involving phase transitions,[21,22] modulated phases,[22] interaction,[23] roughness,[24] chiral structure,[25−27] etc., and also mixed with different compounds.[20,27−32] However, the experimental and the theoretical analysis of penetration of dissolved amphiphiles, like proteins, into the DPPC monolayers, and the effect of protein absorption on the condensed phases of the monolayers is quite new; a review has been presented recently.[33]

The aim of this study is to go a step forward, studying adsorption and monolayer behavior of the exchangeable apolipoproteins CI and AII in a more realistic interface, from a physiological point of view, than the air/highly ionic water interface. Therefore, we prepared a series of experiments to adsorb APO CI and APO AII on a phospholipid (DPPC) monolayer allocated at the air/water interface; there is no salt addition. Here, we will model the lipoprotein hydrophobic/hydrophilic interface by air (hydrophobic) and water, but with DPPC monolayer separating them. At low lateral pressures, the APOs actually penetrate the DPPC monolayer forming binary monolayers. We compressed the monolayers, and observed them using Brewster angle microscopy (BAM). A model is presented to understand the $\Pi-A$ isotherms and the BAM observations. In this model, when the monolayer is formed by penetration at low lateral pressures, a protein-rich phase is formed by lying-down proteins and tilted DPPC molecules. As lateral pressure is increased, a conformational change is developed in the protein molecules of the protein-rich phase, where one α-helix of each chain is desorbed from the interface. However, at the end when compression goes forward, the monolayer expels the protein from the interface in a peculiar way.

Experimental Section

Reagents. Lyophilized human APO CI and APO AII (>98%, PerImmune Incorporation, USA) were solubilized in buffered solutions (pH 8.0) to obtain a concentration of 0.2 mg/mL. They were filtered with 0.22 μm membrane filters before the experiments were carried out. The subphase was ultrapure water (Nanopure-UV, 18.3 MΩ), which was phosphate buffered (sodium phosphate, 99%, Sigma, 20 mm) at pH 8.0. Protein integrity prior to monolayer preparation was done through far-UV circular dichroism,[11,12] and protein concentration was always measured through absorbance measurements.[11,12] DPPC (*rac*-1,2-dipalmitoyl-*sn*-glycero-3-phosphocholine) (>99%) was obtained from Fluka Chemie AG. The DPPC was dissolved in chloroform (99% HPLC grade, Aldrich USA) to form the spreading solution (1 mg/mL).

Monolayer Preparation. All monolayers were prepared on a computerized Nima LB trough (Model TKB 2410A, Nima Technology Ltd., England) using a Wilhelmy plate to measure the lateral pressure, $\Pi = \gamma_o - \gamma$, i.e., the surface tension difference of the clean subphase and that of the covered subphase. Temperature was kept constant at 25 °C with the aid of a water circulator bath (Cole-Parmer 1268-24, USA). The speed of compression was ca. 50 cm^2/min. All experiments were carried out in a dust-free environment.

Preparation of Monolayers of DPPC with APO CI and APO AII. We used two methods to incorporate the APOs into the DPPC monolayer with similar results. In the first one, which we called the injection method, we gently injected at the bottom of the trough right underneath a preformed DPPC monolayer ∼50−250 μL of the buffered solution of the APO under study, with the aid of a needle introduced from outside the barriers to disturb as little as possible the DPPC monolayer. After a waiting time in the range of hours to allow proper adsorption, the compression started or the film was expanded to negligible lateral pressure, and after some relaxation time, it was compressed. In the second method, which we called the dissolution and spreading method, we first incorporated the protein in the subphase by dropping an APO buffered solution into the subphase. After 10−15 min, a specific quantity of DPPC was deposited onto the surface, enough to obtain a required DPPC monolayer pressure, by dropping it dissolved in the spreading solution. In seconds, the pressure increased due to the adsorption of protein, to approximately the same value obtained after the long waiting time when the injection method was used. After 10−15 min, the monolayer was expanded to reach a vanishing pressure, and after 30 min for relaxation, the compression process started.

It is important to mention that far-ultraviolet circular dichroism spectra were obtained for both APOs, when they were dispersed in water, to ensure protein integrity along the time taken for these experiments. Over several hours, up to a couple of days, we observed two minimum spectra values. The first one, around 222 nm, corresponded to α-helix n−π transitions. The second one was around 208 nm and corresponded to both α-helix $\pi-\pi^*$ and random coil $\pi-\pi^*$ transitions. All seemed to indicate that, during the course of the experiments, the secondary structure of the proteins was preserved.

Brewster Angle Microscopy (BMA). BAM observations were performed in a BAM1 Plus (Nanofilm Technologie GmbH, Germany), with a spatial resolution ca. 4 μm. Here, the interface is illuminated at the Brewster incidence angle (∼53°) with a polarized laser beam from a He−Ne laser (632.8 nm). A microscope receives the reflected beam that is analyzed by a

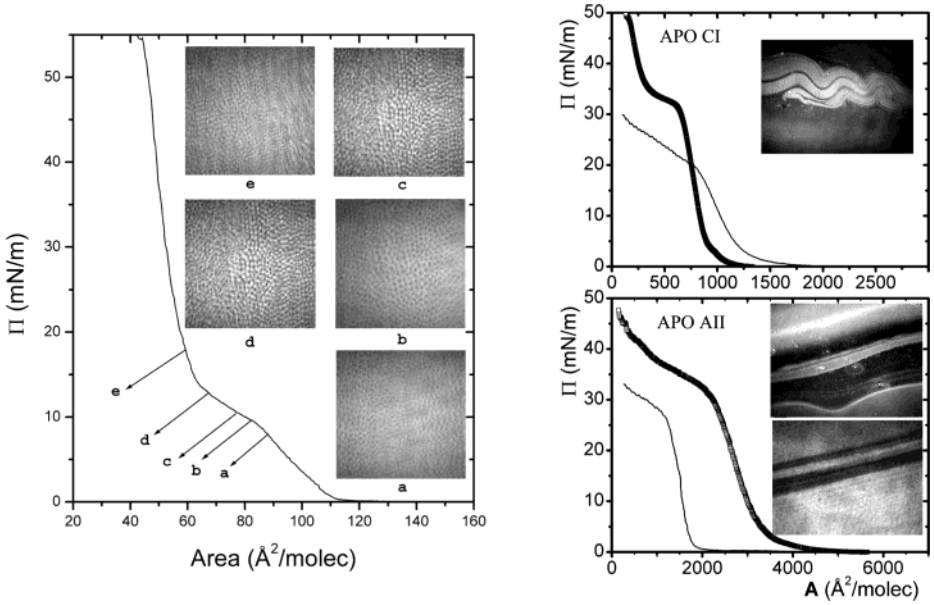

Figure 1. Isotherms Π vs *A* for monolayers of (A, left panel) DPPC spread onto a phosphate buffered water subphase (pH 8.0), at 25 °C; insets show BAM images at different pressures. (B, right panel) APO CI and APO AII isotherms, at 25 °C. Thick lines, proteins spread onto a highly ionic water subphase; thin lines, proteins spread onto a buffered water subphase (pH 8.0) without DPPC coverage. BAM images correspond to L−LC coexistence. In the case of APO AII the upper image corresponds to the highly ionic subphase and the lower image to the uncovered water subphase. Here, a feature not captured by the images is that, close to the borders of the big bright domains (LC phase), it is easy to see streams of the fluid phase L (dark area) flowing.

polarization analyzer, and the signal is received by a CCD video camera to develop an image of the monolayer.

Results and Discussion

One-Component Monolayers. Figure 1A presents a typical isotherm of DPPC monolayer at 25 °C, onto a sodium phosphate buffered water subphase (pH 8.0, 20 mM), presenting two well-known phase transitions: (a) G−L phase transition occurring at $\Pi \sim 0$ mN m^{-1} and (b) LE−LC phase transition at $\Pi \sim 9-12$ mN m^{-1}, $A \sim 65-85$ Å^2 molecule^{-1}. Here, small domains appear and coalesce, along the phase transition, which are easily observed with BAM. The resolution of our BAM images did not allow us to observe the characteristic three armed domains commonly observed in this monolayer. The shape of these domains is determined mainly by three contributions to the free energy: line tension, dipolar interaction, and chiral contribution.[28] At $\Pi \sim 30$ mN m^{-1} the monolayer becomes contrastless, and the collapse is at $\Pi \sim 55$ mN m^{-1} and $A \sim 45$ Å^2 molecule^{-1}.

APOs form Langmuir monolayers upon the surface of a highly ionic water subphase.[11,12] Figure 1B presents typical isotherms for monolayers of APO CI and of APO AII.[11,12] BAM images (insets Figure 1B) show the fluid phase L (dark domain) coexisting with LC phase (bright domains) in a first-order phase transition, which occurs at relatively high lateral pressure for both proteins. In the bright domains of LC phase that are nucleated from the L phase, one α-helix of each chain is desorbed from the interface[11,12,18] as mentioned in the Introduction. More details about the APO isotherms can be found elsewhere.[11,12,18] APOs deposited on the air/water (pH 8.0) interface form Gibbs monolayers, because they are water-soluble proteins. For comparison, we included in Figure 1B the APO CI and the APO AII Gibbs isotherms. The contrast among these isotherms and those for monolayers over highly ionic water subphase is evident. APO CI never reaches high lateral pressures and the L/LC phase transition cannot be observed. Although there is a shoulder in the isotherm at $\Pi \sim 20$ mN m^{-1}, nothing is observed with BAM; a dark gray monolayer is observed all along the compression. APO AII also does not reach high pressures; however, it reaches the L/LC phase transition at $\Pi \sim 30$ mN m^{-1} and can be observed with BAM, as shown in the inset of Figure 1B. As in the case of highly ionic subphase, dark domains correspond to the fluid phase L and bright domains to the condensed LC phase.

Penetration of Apolipoproteins into the DPPC Monolayers. When the APOs are injected beneath the preformed DPPC monolayer, they penetrate the DPPC monolayer after some waiting time. Figure 2 shows some examples of the time needed to achieve a stationary state after the injection of the APOs. Here, the lateral pressure reaches a plateau asymptotically and, apparently, no more APO molecules seem to penetrate the DPPC monolayer. Of course, each run has its own rise time due to the specific way and place where the protein was deposited with the needle, under the monolayer. However, in the pressure rise time curves for both proteins, when proteins were injected beneath the DPPC preformed monolayers at $\Pi \sim 3$ mN m^{-1}, there is a breakpoint that corresponds to a phase transition observed with BAM; the phase transition will be described below. It takes roughly between 1/3 and 4 h to reach the plateau ($\Pi \sim 22$ mN m^{-1}; $\sim 4.541 \times 10^{15}$ molecules) for APO CI, and approximately 8−10 h for APO AII ($\Pi \sim 18$ mN m^{-1}; $\sim 1.729 \times 10^{15}$ molecules). Probably, there are two processes that control the adsorption/penetration of the APOs into the DPPC monolayer. One is related to the transport of the protein to the monolayer (diffusion), and the other is related to the incorporation of the protein at the air/water interface. It seems quite suggestive that the time difference to achieve the stationary state (plateau) in both proteins could be attributed to the fact that APO AII occurs in a dimer and APO CI as a monomer. The dimer is more massive and its diffusion coefficient must be much smaller. In the process of protein incorporation to the interface, hydrophobic interaction with the interface is probably playing an important role. Here, the hydrophobic moment of APO AII (0.415 kcal mol^{-1} residue^{-1})

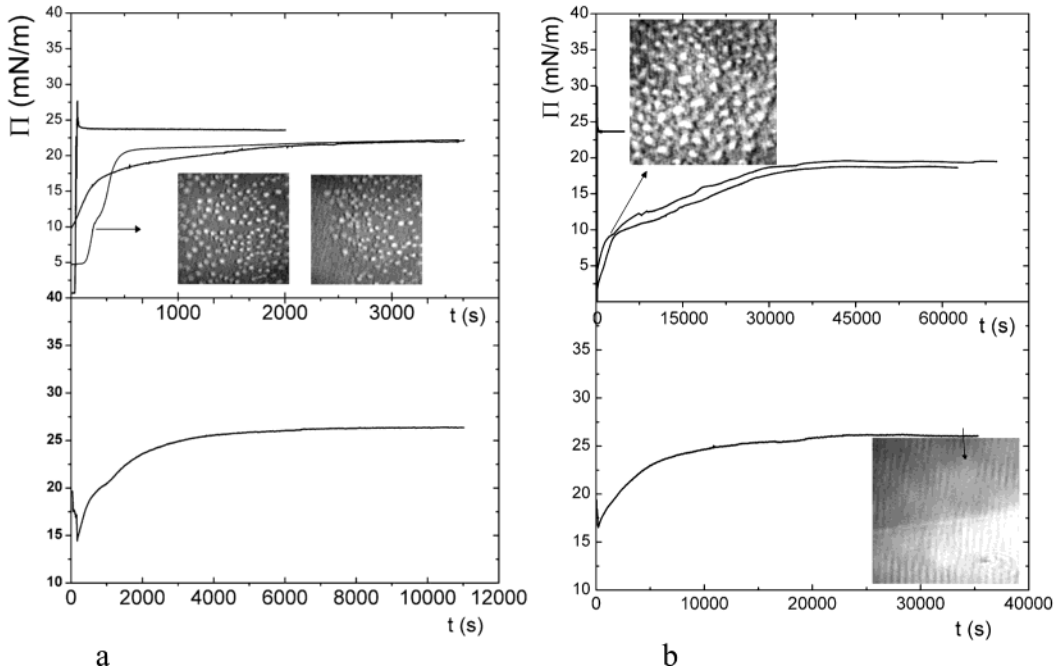

Figure 2. Penetration of apolipoproteins into DPPC monolayer. (a) APO CI and (b) APO AII. Upper panel in both figures: penetration at $\Pi \sim 3$ mN m^{-1}. Lower panel: penetration at $\Pi \sim 20$ mN m^{-1}. Slow growing curves are for penetration by the injection method. Vertical peaks followed by a horizontal line correspond to the dissolution and spread method. Insets are BAM images of the penetrated monolayer at the indicated pressures. In the image on the right for APO CI (upper panel) two domains are clearly seen, one smooth and the other with small bright domains similar to those that appear in the DPPC first-order phase transition.

is slightly lower than the hydrophobic moment of APO CI (0.45 kcal mol^{-1} residue^{-1}). Another contribution could be of electrostatic origin between the DPPC monolayer and the proteins. At the working pH, although the DPPC monolayer is uncharged, it has a dipolar moment that surely interacts with proteins, which on the average are charged, but with a nonhomogeneous charge distribution, too; APO CI is positively charged, while APO AII is negatively charged. In Figure 2, we also show protein adsorption on DPPC when the APOs are injected beneath a DPPC monolayer at $\Pi \sim 20$ mN m^{-1}. For both proteins, there was a transition time where lateral pressure slightly decreases first, before starting to increase on the way to reach a plateau after several hours. The limiting pressure is not what was expected if all the protein would have penetrated the DPPC monolayer. As we will see below, there is a second phase transition between condensed phases in these monolayers, at lateral pressures ca. 24 mN m^{-1} for APO CI and ca. 28 for APO AII. The added protein was enough to pass the phase transition. However, in both monolayers the pressure just reached the onset of the phase transition; pressure never overcame the transition pressure. With BAM, we observed a contrastless monolayer most of the time, except for some cases in APO AII, where it was possible to see some domains with different shades of gray at the onset of the transition.

Figure 2 also shows examples when the dissolution and spreading method was used. Here, the protein−DPPC film is formed in seconds, with a plateau that reaches almost the same lateral pressure as those obtained using the injection method. The spreading of DPPC drives into motion the subphase, and everything seems to indicate that the dissolved protein, through advection, reaches the interface where the DPPC is deposited. It looks like the protein molecules are trapped at the surface. As mentioned in the Experimental Section, it is important to recall that monolayers prepared in this way, after relaxation, produced the same results as those where the injection method was used. However, in the dissolution and spreading method, the film preparation time is particularly reduced.

Area Occupied by APO CI and APO AII in DPPC Monolayers. In this section, we estimate whether all the apolipoprotein injected underneath the DPPC monolayer preformed at $\Pi \sim 3$ mN m^{-1} completely penetrated the monolayer, leaving no free protein in the subphase. Since the protein quantities used in these experiments are low, a direct quantitative analysis turns out to be impractical. Thus, we used an alternative method to estimate the protein in the monolayer. For both proteins, we prepared a DPPC monolayer at $\Pi \sim 3$ mN m^{-1}, which occupied a specific area ($\sim$290 cm^2) in the Langmuir trough. Subsequently, a known quantity of protein was injected directly underneath the monolayer and the barriers were allowed to move, maintaining the lateral pressure constant ($\Pi \sim 3$ mN m^{-1}) to allow protein penetration. We waited the appropriate time for reaching a limiting area as shown in Figure 3. The area increase due to penetration was compared with the area that would occupy the pure APO deposited on highly ionic water subphse, i.e., area per molecule at $\Pi \sim 3$ mN m^{-1} as given by its isotherm, multiplied by the number of APO molecules injected in the subphase. For both proteins, we obtained that some protein is not incorporated in the monolayer, in the range of $\sim$14−15%. Since our binary monolayers are diluted systems (nominal mole fraction, $X_{DPPC} = 0.88-0.99$), we considered as a good approximation that the partial molar areas of each component in the mixture are the same as the molar areas of pure compounds. It may be important to mention that the use of molecular areas of highly ionic subphases could be a problem. However, we found that APOs behaved like geometric rods when deposited on highly ionic water subphases, approximately of the same sizes as those used in biological studies where proteins are worked in low ionic strength solutions.[12,18] On the other hand, molecular areas that we could obtain from isotherms for APOs on a water surface without DPPC coverage would be

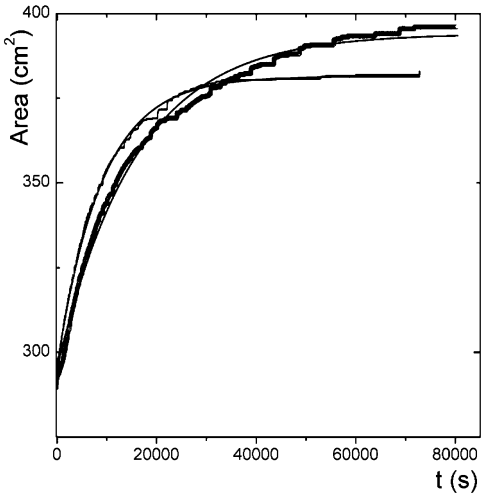

Figure 3. Examples of evolution of area as a function of time at constant pressure ($\Pi \sim 3$ mN m^{-1}) for both proteins, at 25 °C. Thick line, APO AII; thin line, APO CI. The fitting curves for the model given by eq 3 are also shown.

incorrect, since as shown above APOs do not form Langmuir monolayers there, and at certain specific pressures, the monolayer area just reveals the equilibrium between proteins in the monolayer and in the subphase. We expect that if there are some differences in size due to the use of data coming from ionic subphases, those will be small. This issue will be finally solved when AFM studies on APO/DPPC transferred monolayers and grazing X-ray diffraction experiments on binary monolayers have been performed. This study is underway. Therefore, we estimate that around 15% of protein did not penetrate the DPPC monolayer at $\Pi = 3$ mN m^{-1}, probably because APOs are dissolved into the subphase or adsorbed upon the Teflon walls of the trough. Figure 3 presents examples of the evolution of the area as a function of time for both proteins. After ca. 22 h, APO CI reached a limiting area on the average of 401.3 cm^2 and APO AII reached a limiting area on the average of 396.1 cm^2. Differences in area due to protein penetration were on the average of 113.9 cm^2 for the former and of 106.0 cm^2 for the latter.

The area increase due to the penetration of lipoproteins can be easily modeled. The total monolayer area (DPPC + protein) is $A' + A^p$, where A' is the area previously covered by the DPPC (which is a fixed constant) and A^p is the area increase due to protein penetration; i.e., $A^p = a_s N_{mono}$, where a_s is the area per protein and N_{mono} is the number of protein molecules that penetrated the monolayer. We need just two assumptions. The first one is that a_s is a constant along all the penetration process, if lateral pressure is maintained at a low constant value ($\Pi = 3$ mN m^{-1}). Since APOs behave geometrically as rigid rods, each protein that goes to the surface increases the area by a specific amount a_s.[11,12,18] The second assumption is that the rate of area increase, dA^p/dt, due to protein penetration, is proportional to the protein concentration in the subphase, i.e.

$$\frac{dA^p}{dt} = k[P_{sub}] \qquad (1)$$

$[P_{sub}] = N_{sub}/V_{sub}$ is the concentration of the protein in the subphase, N_{sub} is the number of proteins in the subphase, and V_{sub} is the subphase volume. The total number of proteins in the system, N_T, is the sum of the proteins in the subphase plus those in the monolayer, $N_T = N_{sub} + N_{mono}$. Then, the change of total area in the trough per unit time is

$$\frac{d}{dt}(A' + A^p) = \frac{dA}{dt} = k[P_{sub}] = \frac{d}{dt}(a_s N_{mono}) = \frac{k(N_T - N_{mono})}{V_{sub}}$$

From here, we obtain a first-order differential equation:

$$\frac{dN_{mono}}{dt} + \frac{k}{a_s V_{sub}} N_{mono} = \frac{k}{a_s V_{sub}} N_T \qquad (2)$$

Solving the equation, and multiplying by a_s, we obtain

$$A^p(t) = a_s N_T + a_s(N_o - N_T) \exp\{-[k/(a_s V_{sub})]t\} \qquad (3)$$

Here, N_o is the number of protein molecules in the monolayer at $t = 0$. Equation 3 has been used to fit the curves for the area of the penetrated monolayer vs elapsed time such as those presented in Figure 3; the agreement is very good. From the fittings, the k values are the following: 6.12×10^{25} Å^5 s^{-1} molecule^{-1} for APO CI and 13.6×10^{25} Å^5 s^{-1} molecule^{-1} for APO AII. These k values indicate that APO AII penetrates the DPPC monolayer more readily than APO CI. Hydrophobic moment and subphase diffusion, as mentioned above, suggested that APO CI should perform better. Since constant k measures the capability of protein incorporation to an interface and consequently the interface−protein interaction, then the results obtained for k show that those properties do not estimate properly the capability of protein incorporation to an interface.

A different way to support that APO AII interacts stronger with DPPC than APO CI is using the experimental data for protein adsorption with different interfaces, keeping the area for spreading constant. We have observed (data not shown) that the adsorption of APO AII at the air/water interface is not as efficient as when it is covered with DPPC, i.e., equilibrium Π is larger in the latter case; this occurs even at low lateral pressures. In the case of APO CI, the adsorption is similar between the air/water interface and the DPPC-covered interface at low lateral pressures, i.e., below the L/LC phase transition. In both cases, above the L/LC phase transition the DPPC coverage is necessary to maintain the protein at the air/water interface. On the other hand, when a high ionic strength subphase is used, all protein is expelled from the subphase to the air/water interface (Π is even larger in this case), as in a salting-out effect, allowing the formation of a Langmuir monolayer.[12,18]

Phase Transitions. DPPC penetrated monolayers were isothermically compressed after an expansion to a vanishing pressure and some waiting time for relaxation. Figure 4 presents the isotherms for the APO CI/DPPC and APO AII/DPPC binary systems, for different quantities of added protein, at 25 °C. As in three-dimensional systems, we do not expect clear-cut phase transitions because our monolayers are binary systems. Therefore, phase transitions occur along a relatively wide range of lateral pressures. In the isotherms, along the compression, three phase transitions are clearly observed in both binary systems. There is a first-order phase transition of not much interest here, between a contrastless binary gas and a binary contrastless liquid phase (L). This transition occurs at $\Pi \sim 0$, where the isotherm is horizontal, and ends up at $A \sim 140-160$ Å^2 molecule^{-1}, depending on the quantity of added protein.

On compression, the next phase transitions correspond to transitions between condensed phases: A clear kink reveals the start of a phase transition at $\Pi \sim 8-11$ mN m^{-1} and densities at $A = 100-125$ Å^2 molecule^{-1} depending on the amount of

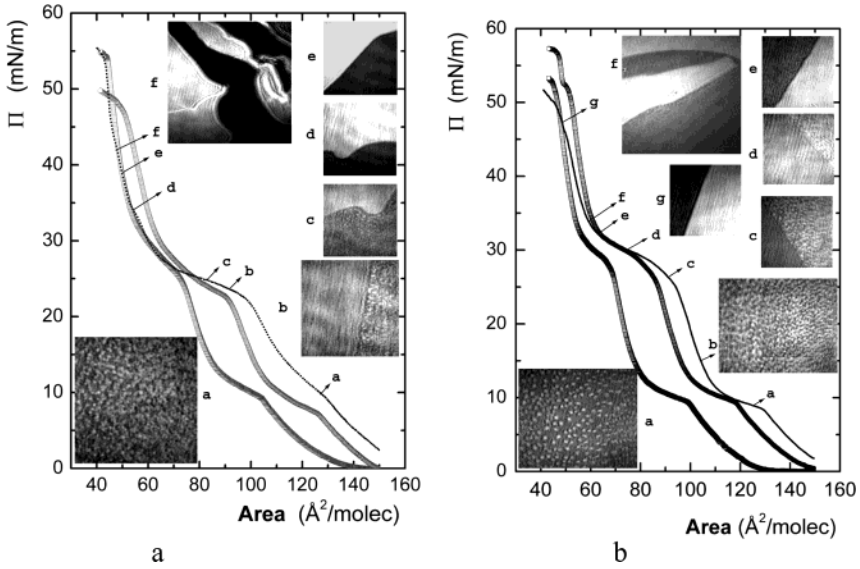

Figure 4. Π vs *A* isotherms for (a) DPPC/APO CI (nominal monolayer mole fraction, from left to right: $X = 0.04, 0.05, 0.12$) and (b) DPPC/APO AII (nominal monolayer mole fraction, from left to right: $X = 0.01, 0.02, 0.03$). Insets show BAM images at different lateral pressures.

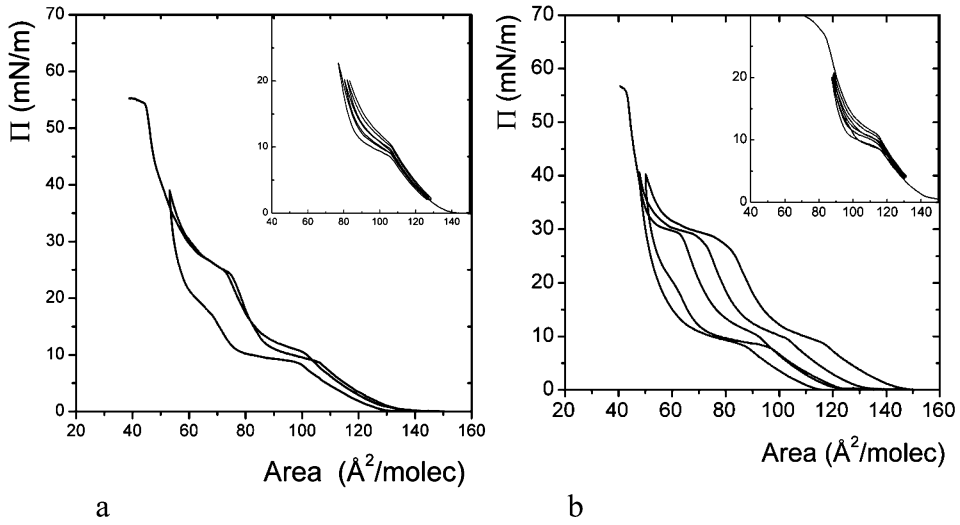

Figure 5. Cycles of compression and decompression for DPPC/APO CI (a) and DPPC/APO AII (b) monolayers.

added protein. BAM images reveal that at the onset of the phase transition solid domains are nucleated from the L phase. These are small domains, very similar to those presented in the phase transition of DPPC at 9−12 mN m^{-1}. As pressure increases by a small amount, these phase domains coalesce, forming an extended film with a rough texture; it seems like a wrinkled surface. There is a second kind of phase domains also nucleated from the L phase and made up of contrastless domains. They present a homogeneous texture that forms smooth surfaces. These domains are not abundant along the monolayer. At the onset of phase transition, the metastable L phase is flowing and rapidly disappearing as pressure increases. The gray hue of the smooth domains, similar to that of L phase, is slightly darker than the gray hue of the rough domains. However, as pressure increases, the two kinds of domains can be clearly distinguished. Both kind of domains recall the texture of $\alpha-\beta$ phases in 3D binary alloys, where microstructure depends on the specific path followed to get the two phases. Examples of this transition are presented in the upper panel insets of Figure 2 and in Figure 4. As pressure increases, there is another transition that seems to modify just one of the phases. It starts with a pronounced shoulder at $\Pi \sim 24-27$ mN m^{-1} and $A = 65-100$ Å^2 molecule^{-1} for DPPC/APO CI, and at $\Pi \sim 28-31$ mN m^{-1} and $A = 60-90$ Å^2 molecule^{-1} for DPPC/APO AII, depending on the quantity of added protein, as shown in the isotherms of Figure 4. In this transition, there is a considerable loss of area per particle. The BAM images reveal that the smooth contrastless domains coming from the previous transition, at the onset of this transition, start to transform from gray to very bright; the rough phase domains seems the same as before the transition, but due to the nonlinear contrast gain of the microscope they appears as dark gray. The phase transitions just described are reversible and reproducible, as can be observed in the cycles of compression and decompression presented in Figure 5 for both proteins. The area per particle change and the reversibility with hysteresis in these phase transformations seem to indicate that they correspond to first-order phase transitions.

As the compression process is carried out, above the phase transitions just described, at $\Pi \sim 49$ mN m^{-1} for DPPC/APO CI and at 47.5−49 mN m^{-1} for DPPC/APO AII, the bright domains melt away leaving only dark gray domains in all the field of view. Without the bright domains as a contrast, all the field of view takes on a light gray hue as before the phase transition; see Figure 6. This hue of gray is similar to that of pure DPPC monolayers at this lateral pressure. This process that is like another phase transition is reversible, although

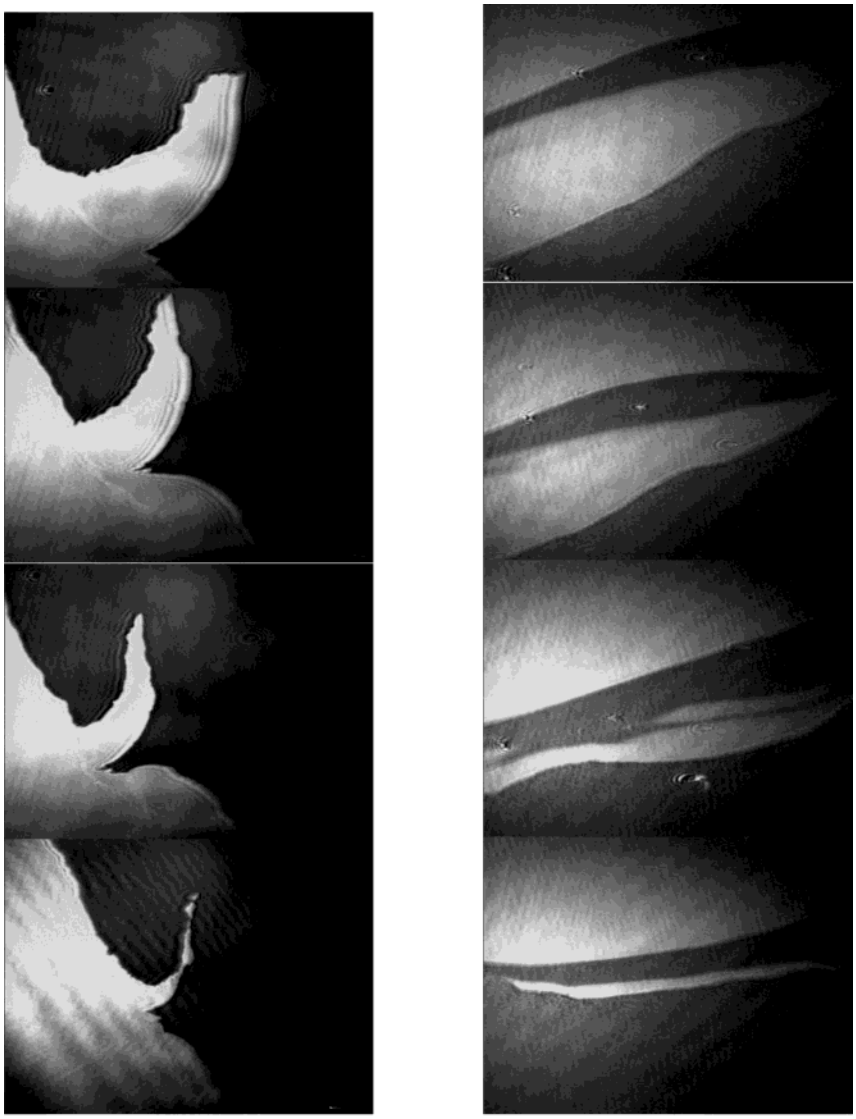

Figure 6. BAM images of bright domains melting away. The dark gray domain ends up covering all the field of view. DPPC/APO CI (a) and DPPC/APO AII (b).

difficult to be studied, because it is close to the collapse and the isotherm is quite steep there. We will discuss this later.

An interpretation of the events just described along the compression can be given taking into account on one hand that DPPC is an amphiphile with a bulk hydrophilic head and two long hydrophobic tails, and on the other hand that both proteins have been previously modeled.[11,12,18] APO CI presents two-amphiphilic α-helices of approximately 28.5 and 40.5 Å in length bonded by a loose hinge, and APO AII presents two-amphiphilic chain α-helices bonded at position 6, where each chain has two α-helices also bonded by a loose hinge, of approximately 31.5 and 54 Å in length. At pressures below $\Pi \sim 10$ mN m^{-1}, i.e., in the L phase, the proteins and the DPPC molecules form an isotropic liquid mixture, where the protein molecules are traveling in a landscape of close energy minimum configurations, where the different protein configurations have the restriction of being laid down along the long axis of the α-helices on the subphase; the tails of DPPC are correlated probably as in the L pure DPPC monolayer. The hydrophilic faces of the α-helices and the heads of the DPPC must be in contact with the water subphase, and the hydrophobic faces and the DPPC tails must be oriented toward the air. Here, at low lateral pressures, the area covered by the DPPC/APO monolayer is roughly the sum of the areas covered by the molecules of protein and of DPPC, as in their pure state, as shown before. Along the phase transition, at $\Pi \sim 10$ mN m^{-1}, two phase domains are formed. One is formed by the coalescence of small domains, which are very similar to those observed in the pure DPPC monolayer and probably rich in DPPC. These domains have a rough texture in BAM images, resembling the pure DPPC texture. The second kind of less abundant domains has a smooth texture and forms a phase that is probably rich in protein. The DPPC molecules in the rough domains are probably tilted and orientationally ordered, and the α-helices in the smooth domains are lying down on the water surface (Figure 7). In the next phase transition, $\sim$24−31 mN m^{-1} depending on the protein content, a big change of area per particle starts. Here, the rough phase domains leave its reflectivity almost without change, revealing that the DPPC chain tilting has not changed too much. However, the smooth phase domains become very bright. Taking into account that the BAM reflectivity formula is a quadratic function on the film thickness, and the desorbing behavior of APOs in pure monolayers on a highly ionic subphase at about the same lateral pressures, it is quite possible that the protein molecules

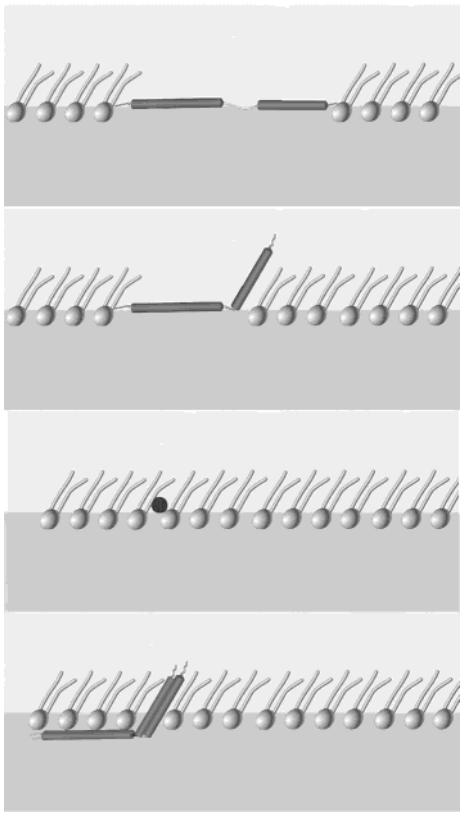

Figure 7. Model for the binary monolayer. From upper panel to lower panel: (a) Model for the smooth domains rich in protein above the phase transition that occurs ∼9−12 mN m^{-1}; (b) Model for protein-rich domains above the phase transition that occurs ∼24−31 mN m^{-1}. Model for the dark gray domain covering all the field of view in the BAM images, after the melting away of the bright domains: (c) APO CI oriented parallel to the air/water interface; (d) APO AII partially expelled from the air/water interface.

suffer a conformational change also in this binary system. APO monolayers on a highly ionic subphase, above the L/LC phase transition,[18] present a diffraction peak at $q_z \neq 0$ for the case of APO CI, indicating that the order goes only in one direction, with an arrangement of rows formed by desorbed tilted α-helices and rows of α-helices parallel to the surface, at the water/air interface. q_z is the momentum transfer vector in the vertical direction. APO AII presents an arrangement of rows of desorbed tilted α-helices and α-helices parallel to the surface. This arrangement exhibited two diffraction peaks: one is associated with the tilted helix order ($q_z \neq 0$), and the other is associated with the order between rows formed by the α-helices lying down on the surface. In the present case of DPPC-covered water/air interface, one α-helix segment (APO CI) or two α-helix segments (APO AII) could desorb from the subphase, aligning them following the tilting of the DPPC tails. This could explain the large area loss in the isotherms and the brightness of the smooth domains (Figure 7). A rough estimate of the area lost along the whole transition is consistent with the desorption.

The most difficult point to be explained is related to the events that occurred afterward, i.e., when the brilliant smooth phase domains melt away. Here, it looks like as if the monolayer loses film thickness and, at the end, the reflectivity of the monolayer seems similar to that of domains rich in DPPC. The only solution to explain the thickness lost is that the monolayer pushes the protein from the air/water interface. Evidence of this fact is that the area per molecule at the collapse, for the binary monolayers of both proteins, is very close to the area per molecule for the collapse of pure DPPC monolayer; see Figures 4 and 1A. If this is a phase transition, it is a peculiar transition between a 2D monolayer and a 3D structure, which occurs in a continuous form. However, if proteins are expelled into the subphase or into air, without any constraint, they could have the α-helix faces incorrectly exposed to air or to water, i.e., hydrophobic faces exposed to the DPPC tails and hydrophilic faces exposed to air (protein expelled into air) or hydrophilic faces close to the DPPC heads and hydrophobic faces exposed to water (protein expelled into the subphase). It is difficult to predict if a change in reflectivity can be observed in the domains after the expulsion of the proteins. However, as mentioned before, there are no reflectivity differences in BAM images along the field of view. On the other hand, there could be an intermediate possibility; this can be observed in our model in Figure 7. Here, when APO CI molecules are expelled from the air/water interface, they recover their unbent conformation leaving the interface to be allocated just above the heads and between the tails of the DPPC amphiphiles. The required space for allocating a rod (protein) between the DPPC lattice is the diameter of an α-helix, i.e., ∼5 Å. Given the big size of the DPPC heads, this probably introduces just a small defect in the tilted−condensed orientationally ordered DPPC phase. However, the DPPC molecules just surrounding the incorporated rods probably would be highly distorted. Until now the order of phospholipid heads has been unknown, but among the expected arrangements there are several that could not be distorted much by including an α-helix rod as proposed.[35] In this way, the hydrophilic faces of the proteins are interacting with the heads and the hydrophobic faces with the tails. The case of APO AII is more difficult to explain. Here, we suspect that the protein is expelled from the water/air interface in a very peculiar way; since it has two chains, the way of expulsion proposed for APO CI would distort the DPPC lattice too much. Therefore, we propose that two α-helices still are tilted, but the other two α-helices are expelled from the interface to be allocated beneath the monolayer as shown in Figure 7. Here a little twisting of the horizontal chains could make the hydrophobic faces hidden to avoid direct contact with the subphase.

Conclusion

We have studied binary systems made up of an apolipoprotein and phospholipid. We found that these systems present two phase transitions at high lateral pressure and have presented a model to understand them. In this model, in the protein-rich domains, protein is lying down upon the air/water interface in the L phase. As pressure increases, there is a phase transition where α-helices desorb from the interface following the DPPC tilting. When lateral pressure is increased even more, protein seems to be squeezed from the phospholipid monolayer in a peculiar way, as in the case of APO AII, or it could be still there modifying the DPPC monolayer structure, as in the case of APO CI. Since these processes at high lateral pressures are not completely understood, grazing incidence X-ray diffraction and atomic force microscopic observation of Langmuir−Blodgett films of transferred monolayers are indispensable. These studies are underway. The important biological implications of this work could be directly related to the physiological function of lipoproteins. First, the location of the APOs in the lipoprotein particles could be associated with the lateral pressure in the surface of these particles. Second, the conformational structure of the APOs present in the lipoprotein particles could also be related to the lateral pressure in these particles. Third, there could be a process using the lateral pressure along the maturation of lipoproteins that could control the position and conformational structure of the APOs in the lipoprotein particle.

Acknowledgment. We acknowledge the technical help in running the isotherms and BAM observations of S. Ramos and the technical support of B. Delgado-Coello and C. Garza. Financial support provided by CONACYT (36680-E and PMB) and DGAPA-UNAM grants (IN 212301, IN113601).

References and Notes

(1) Despres, J. P.; Lemieux, I.; Dagenais, G. R.; Cantin, B,; Lamarche, B. *Atherosclerosis* **2000**, *153*, 263.
(2) Segrest, J. P.; Jones, M. K.; De Loof, H.; Dashti, N. *J. Lipid Res.* **2001**, *42*, 1346.
(3) Segrest, J. P.; Jones, M. K.; De Loof, H.; Brouillette, C. G.; Venkatachalapathi, Y. V.; Anantharamaiah, G. M. *J. Lipid Res.* **1992**, *33*, 141.
(4) Stein, O.; Stein, Y. *Atherosclerosis* **1999**, *144*, 285.
(5) Hajjar, K. A.; Nachman, R. I. *Annu. Rev. Med.* **1996**, *47*, 423.
(6) Plutzky, J. *Curr. Opin. Cardiol.* **2000**, *15*, 416.
(7) Yokoyama, S. *Biochim. Biophys. Acta* **1998**, *1392*, 1.
(8) Borhani, D. W.; Rogers, D. P.; Engler, J. A.; Brouillette, C. G. *Proc. Natl. Acad. Sci. U.S.A.* **1997**, *94*, 12291.
(9) Mehta, R.; Gantz, D. L.; Gursky, O. *Biochemistry* **2003**, *42*, 4751.
(10) Bolaños-Garcia, V. M.; Soriano-Garcia, M.; Mas-Oliva, J. *Mol. Cell. Biochem.* **1997**, *175*, 1.
(11) Bolaños-Garcia, V. M.; Ramos, S.; Castillo, R.; Xicohtencatl-Cortes, J.; Mas-Oliva, J. *J. Phys. Chem. B* **2001**, *105*, 5757.
(12) Bolaños-Garcia, V. M.; Mas-Oliva, J.; Ramos, S.; Castillo, R. *J. Phys. Chem. B* **1999**, *103*, 6236.
(13) Weisgraber, K. H.; Newhouse, Y. M.; McPherson, A. *J. Mol. Biol.* **1994**, *236*, 382.
(14) Rozek, A.; Buchko, G. W.; Kanda, P.; Cushley, R. J. *Protein Sci.* **1997**, *6*, 1858.
(15) Rozek, A.; Buchko, G. W.; Cushley, R. J. *Biochemistry* **1995**, *34*, 7401−7408.
(16) Buchko, G. W.; Rozek, A.; Zhong, Q.; Cushley, R. J. *Pept. Res.* **1995**, *8*, 86.
(17) Brewer, H. B.; Lux, S. E.; Ronan, R.; John, K. M. *Proc. Nat. Acad. Sci. U.S.A.* **1972**, *69*, 1304.
(18) Ruiz-Garcia, J.; Moreno, A.; Brezesinski, G.; Möhwald, H.; Mas-Oliva, J.; Castillo, R. *J. Chem. Phys.* **2003**, *107*, 11117.
(19) Kaganer, V. M.; Möhwald, H.; Dutta P. *Rev. Mod. Phys.* **1999**, *71*, 779.
(20) Krasteva, N.; Vollhardt, D.; Brezesinski, G.; Mohwald, H. *Langmuir* **2001**, *17*, 1209.
(21) Albrecht, O.; Gruler, H.; Sackmann. E. *J. Phys. (Paris)* **1978**, *39*, 301.
(22) McConnell, H. M. *Annu. Rev. Phys. Chem.* **1991**, *42*, 171.
(23) Nandi, N.; Vollhardt, D. *J. Phys. Chem. B* **2002**, *106*, 10144.
(24) Schief, W. R.; Hall, S. B.; Vogel, V. *Phys. Rev. E* **2000**, *62*, 6831.
(25) Weiss, R. M.; McConnell, H. M. *J. Phys. Chem.* **1985**, *89*, 4453.
(26) Amador Kane, S.; Compton, M.; Wilder, N. *Langmuir* **2000**, *16*, 6447.
(27) Kruger, P.; Lösche, M. *Phys. Rev. E* **2000**, *62*, 7031.
(28) Weiss, R. M.; McConnell, H. *J. Phys. Chem.* **1985**, *89*, 4453.
(29) Wüstneck, N.; Wüstneck, R.; Fainerman, V. B.; Miller, R.; Pison, U. *Colloids Surf. B* **2001**, *21*, 191.
(30) Amador Kane, S.; Floyd, S. D. *Phys. Rev. E* **2000**, *62*, 8400.
(31) Sundaram, S.; Ferri, J. K.; Volhardt, D.; Stebe, K. J. *Langmuir* **1998**, *14*, 1208.
(32) Fainerman, V. B.; Zhao, J.; Vollhardt, D., Makievski, A. V.; Li, J. B. *J. Phys. Chem. B* **1999**, *103*, 8998.
(33) Volhardt, D.; Fainerman, V. B. *Adv. Colloid Interface Sci.* **2000**, *86*, 103.
(34) Krüger, P.; Lösche. M. *Phys. Rev. E* **2000**, *62*, 7031.
(35) See Figure 26 of ref 12.